

Molecular dynamics simulations of surface-induced ordering in a nematic liquid crystal

J. Stelzer,* P. Galatola, and G. Barbero

Dipartimento di Fisica, Politecnico di Torino, and Istituto Nazionale di Fisica della Materia, Corso Duca degli Abruzzi 24, I-10129 Torino, Italy

L. Longa

Centro Internacional de Fisica da Materia Condensada, Universidade de Brasilia, Caixa Postal 04667, 70919-970 Brasilia, Distrito Federal, Brazil

and Department of Statistical Physics, Jagellonian University, Reymonta 4, Kraków, Poland

(Received 12 July 1996)

By means of a molecular dynamics simulation, we show that a uniaxial nematic liquid crystal may exhibit an unusual ordering that appears within a few molecular lengths from a rough surface. In contact with the surface, a smectic-*C* layering is induced. Moving towards the bulk, the smectic order disappears and a decrease of the uniaxial orientational order below the bulk value occurs. The intermediate region between the surface-induced smectic-*C* ordering and the bulk nematic is characterized by a considerable degree of biaxiality. Correspondingly, the director orientation undergoes a strong distortion close to the surface. [S1063-651X(97)02601-9]

PACS number(s): 61.30.Cz

Nematic liquid crystals consist of elongated molecules whose centers of mass are distributed in a liquidlike manner, but whose average orientation presents long-range order [1]. This average orientation locally defines the nematic director \mathbf{n} . The orienting effects of external fields and surfaces can produce inhomogeneous director fields. The distortions occur on a macroscopic scale and are well described by a continuum elastic theory in terms of bulk elastic constants [2–4]. Additional surface elastic constants were proposed on the basis of symmetry considerations [5], and shown to be nonzero for certain molecular interactions [6]. Among these, the K_{13} constant, giving the energy density $K_{13}\nabla\cdot(\mathbf{n}\nabla\cdot\mathbf{n})$, poses severe mathematical difficulties, since it renders the total elastic energy of a distorted sample unbounded from below [7]. Various approaches have been suggested to overcome this problem. One of the solutions gives rise to strong distortions localized on a molecular range close to the surface [7,8]. This conclusion has been opposed by some authors, who claim that no surface distortions should be present [9,10]. All these descriptions rely on continuum theories that are strictly valid only at a macroscopic level. Therefore, a proper investigation of the existence of a subsurface deformation should be based on a molecular approach. To this purpose, we use a molecular dynamics simulation, which allows us to take into account all the details of the molecular interactions. In this paper, we show that indeed strong deformations in the director field can occur. The model interaction that we use is the well-established Gay-Berne pair potential [11]. As in the case of the induced dipole-induced dipole interaction of the Nehring-Saupe type [6], it depends not only on the orientations of the two molecules, but also on their orientation with respect to the separation vector. It is

this dependence that has been shown to be connected with a nonzero K_{13} and subsurface deformations [12].

The Gay-Berne potential describes interactions between elongated, axially symmetric molecules. Two parameters χ and χ' describe the anisotropy of the molecular shape and of the interaction energy, respectively. To simulate a nematic liquid crystal phase we choose $\chi=0.8$ and $\chi'=0.3167$, which were previously used by de Miguel *et al.* [13] in their evaluation of the phase diagram. All physical quantities are normalized to the molecular diameter and the interaction energy [14].

We model the anisotropic surface interaction by a one-particle potential V_{surf} that consists of two parts $V_{\text{pos}}(\mathbf{r}_i)$ and $V_{\text{orient}}(\mathbf{e}_i)$, depending on the position \mathbf{r}_i and orientation \mathbf{e}_i of the molecule, respectively,

$$V_{\text{surf}} = 4 \epsilon_{\text{surf}} V_{\text{pos}}(\mathbf{r}_i) V_{\text{orient}}(\mathbf{e}_i). \quad (1)$$

Here ϵ_{surf} represents the strength of the surface potential. In our simulations it takes the value of 1 (in reduced units), just as the strength of the Gay-Berne bulk energy.

The positional part of the interaction between the surface and the molecules is taken as a one-dimensional Lennard-Jones potential along the z axis (surface normal). In order to model a rough interface we used a surface sinusoidally modulated along the x and y directions,

$$V_{\text{pos}} = \left(\frac{\sigma}{z + z_0 + a_0 \sin(k_x x) \sin(k_y y)} \right)^{12} - \left(\frac{\sigma}{z + z_0 + a_0 \sin(k_x x) \sin(k_y y)} \right)^6. \quad (2)$$

Here z_0 denotes the average position of the surface, $\sigma=1$ (in reduced units), and a_0 , k_x , and k_y are the amplitude and the wave vector components of the undulated surface, respectively. We take $a_0=1$ (in reduced units). In order to avoid

*On leave from Institut für Theoretische und Angewandte Physik, Universität Stuttgart, Pfaffenwaldring 57, D-70550 Stuttgart, Germany.

difficulties with periodic boundary conditions, we choose the wave vector components in such a way that an integer number of periods of the surface profile fits into the simulation box. The lateral dimensions of the box are equal to 8.69 and $k_x = k_y = 5.06$, corresponding to a surface period of $1/7$ of the box length. The height of the box is 32.9.

The orientational part of the surface potential is modeled by a Rapini-Papoular-like [15] angular dependence

$$V_{\text{orient}} = 1 + \chi_{\text{surf}}^2 (\mathbf{e}_i \cdot \mathbf{k})^2, \quad (3)$$

where \mathbf{k} is the surface easy axis, which we take in the (x, z) plane. χ_{surf} is the anisotropy of the surface, which we choose equal to 3.

The initial configuration is a nematic bulk containing 810 particles, with the director along the z axis. Two surface potentials of the type given above are placed at the top and bottom of the central simulation box. The easy axes are parallel, in order to avoid elastic distortions, and are characterized by the tilt angle ϑ_e with respect to the z axis. In the lateral dimensions [(x, y) plane], periodic boundary conditions are imposed. For the integration of the molecular equations of motion an extension of the Toxvaerd algorithm [14,16] is used. Temperature and pressure are adjusted to 1.00 and 4.35, respectively. This is within the lower range of the Gay-Berne nematic phase.

For an equilibration period of 40 000 time steps (time step of 10^{-3} in reduced units), the walls are left free to move along the z direction, in order to adjust the pressure to its bulk nematic value. The equilibration is followed by other 20 000 time steps with fixed walls, to evaluate the z dependence of the particle density and of the nematic tensor order parameter $\mathbf{Q} = \langle \mathbf{Q}_i \rangle = 3/2 (\langle \mathbf{e}_i \otimes \mathbf{e}_i \rangle - 1/3 \mathbf{I})$. Here $\langle \rangle$ denotes time and particle average and \mathbf{I} is the identity tensor. The particle average at a given z coordinate is performed by weighing the \mathbf{Q}_i tensor of the i th particle with a Gaussian factor $\propto \exp[(z - z_i)^2 / 2s^2]$, where z_i is the z coordinate of the i th particle. We take s equal to $1/12$ th of the box height: this value is sufficiently small with respect to the observed spatial variations of \mathbf{Q} ; we checked that by reducing s the same profiles are obtained. In the principal reference frame $\mathbf{Q} = \text{diag}(-S/2 - P/2, -S/2 + P/2, S)$, where S (P) is the uniaxial (biaxial) order parameter [17], and the third axis gives the nematic liquid crystal director orientation. During the production period of the data, we perform additional averages over smaller amounts of time in order to check the stationarity of the profiles. This stationarity is also confirmed by the fact that varying the initial conditions (e.g., the initial orientations of the molecules) we obtain the same profiles.

A typical snapshot of the molecular configuration under stationary conditions is shown in Fig. 1. The molecules are projected onto the (x, z) plane, which contains the surface normal z and the easy axis direction \mathbf{k} , having the tilt angle $\vartheta_e = 70^\circ$ with respect to z . At both surfaces, two pronounced smectic layers are present. They correspond to molecules that are situated at the bottom and top of the undulated surfaces; only a few molecules occupy intermediate positions. The average orientation inside these layers almost coincides with the easy axis. Due to the roughness of the surface, the smectic order disappears immediately when moving away from the surfaces, leaving a nematic liquid crystal structure

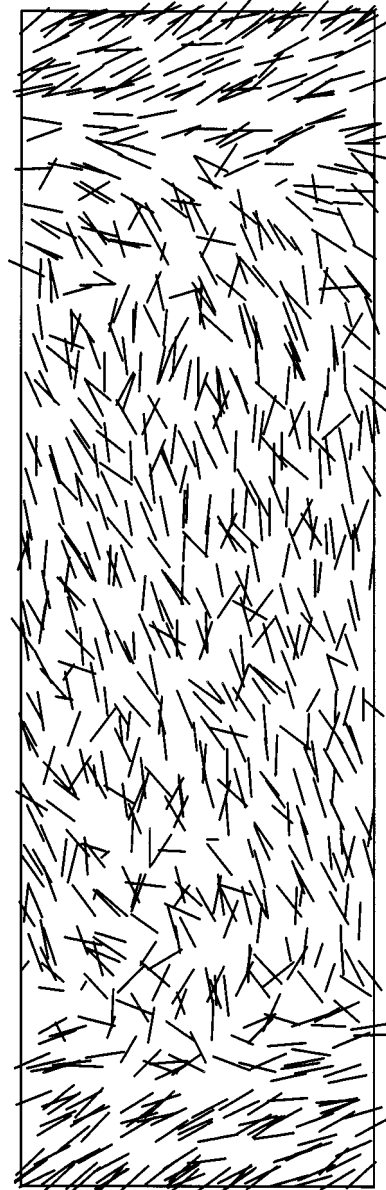


FIG. 1. Snapshot of the molecular configuration after an equilibration time of 40 000 time steps. The molecules are projected onto the plane of the normal to the surfaces z and the easy axis \mathbf{k} . The easy axis is tilted by $\vartheta_e = 70^\circ$ with respect to z .

within the bulk. Furthermore, the average molecular orientation in the bulk significantly differs from the easy axis yielding strong subsurface distortions in the range of 3–4 molecular lengths.

Figure 2 reports the density profile corresponding to the above discussed snapshot: it shows the existence of a stable, surface-induced smectic- C layering. The lateral pair distribution function g_2 with respect to the molecular separation in plane, evaluated for molecules lying within the first density peak closest to the lower surface (see Fig. 2), shows a liquidlike behavior in plane (cf. Fig. 3), confirming the smectic- C ordering of the surface layers. This smectic structure is expected to increase the orientational order as well. Indeed, Fig. 4 reveals such a behavior: the nematic liquid crystal order parameter nearly reaches its saturation value at

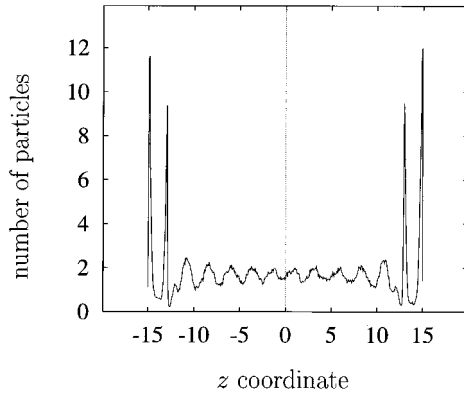


FIG. 2. Number of particles as a function of the normal coordinate z corresponding to Fig. 1. The number of particles is defined as the time averaged number of molecules in each of 500 equidistant slabs normal to the z axis in which the cell has been divided.

the surfaces. In the bulk, the order parameter is equal to its value for an infinite sample. However, remarkably, a depression of the order appears in a region separating the surface-induced smectic from the bulk nematic. Such a “melting” has been suggested to occur close to a rough surface [18,19]. For any surface tilt angle ϑ_e , the profile of the order parameter shows a similar nonmonotonic behavior. It is more pronounced for higher angles, and it is accompanied by a correspondingly higher induced biaxiality. Such a surface-induced biaxiality was first considered in [17] and studied in the framework of a low density Onsager approximation in [20].

The subsurface deformation is apparent in Fig. 5, which displays the profile of the nematic liquid crystal director represented on the unit sphere. In the intermediate region, where the nematic liquid crystal order is reduced, the director undergoes a rapid distortion from the surface angle to an almost homeotropic orientation. This reorientation occurs in the vicinity of the (x,z) plane and is more abrupt for higher surface tilt angles ϑ_e .

To conclude, by means of a molecular dynamics simulation, we have analyzed the behavior of a nematic liquid crystal close to a rough surface. Our analysis has shown that a rather strong change in the director orientation occurs. This

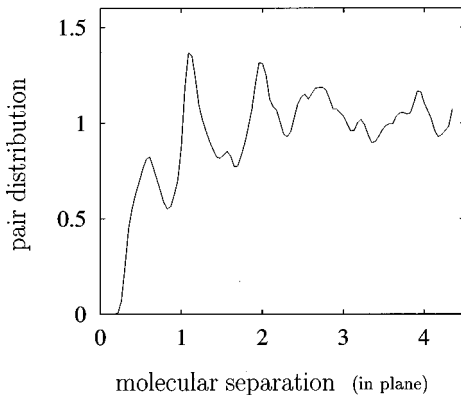


FIG. 3. Pair lateral distribution function g_2 vs molecular separation for the plane closest to the lower surface corresponding to Fig. 1.

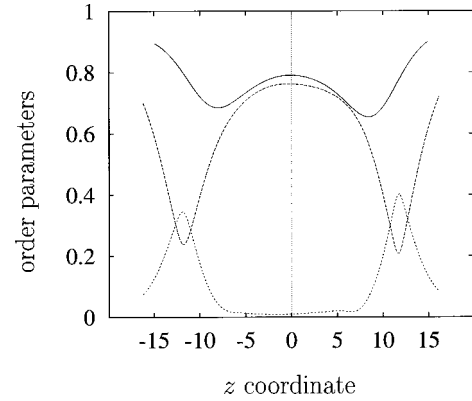


FIG. 4. Order parameters as a function of z . Full line: uniaxial order parameter S for the surface tilt $\vartheta_e=20^\circ$. Dashed lines: uniaxial order parameter S (upper curve) and biaxial order parameter P (lower curve) for $\vartheta_e=70^\circ$. For $\vartheta_e=20^\circ$ the biaxiality is negligible.

reorientation is accompanied by a change in the positional and orientational ordering. The surface, even if rough, induces a smectic layering, as experimentally found [21,22]. A positional and orientational “melting” then occurs. The latter has been theoretically suggested and analyzed by means of a Landau approach in [18]. Its consequences on the anchoring properties have been experimentally investigated in [19]. Our results are qualitatively independent of the surface interaction law. We checked it by considering different surface anisotropic potentials and roughnesses. As long as the surface distortion is connected with the smectic ordering, we also expect that the detailed form of the bulk intermolecular potential does not play a determinant role. The existence of a subsurface deformation was first proposed in connection with the splay-bend elastic constant K_{13} [8]: there it is shown that the subsurface deformation is $\Delta\vartheta = \vartheta_{\text{bulk}} - \vartheta_{\text{surface}} = -(K_{13}/2K_{11})\sin(2\vartheta_{\text{surface}})$. For our Gay-Berne potential $K_{13} \sim -0.03K_{11}$ [14]: this would give a maximum distortion $\Delta\vartheta \sim 2^\circ$ toward the planar orientation. This is much smaller than the values obtained in our simulation and

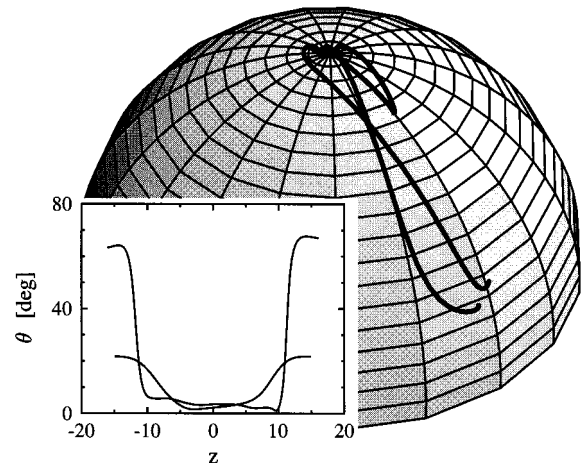


FIG. 5. Unit sphere representation of the path followed by the director along the z axis for $\vartheta_e=20^\circ$ and $\vartheta_e=70^\circ$. The inset shows the profiles of the polar angle ϑ vs z .

in the wrong direction. However, recently it has been shown that for small distortions the most important contribution to $\Delta\vartheta$ actually comes from the homogeneous part of the free-energy density [23]. In the framework of [23], we have numerically evaluated $\Delta\theta$ for our Gay-Berne potential, finding $\Delta\theta \sim -3^\circ$: this is now in the correct direction, but still too small. Hence we conclude that the smectic layering and the orientational melting play a predominant role. Our analysis shows that an elasticlike description near a boundary [8,23] is not satisfying. This is not so surprising, since the surface behavior is expected to strongly depend on the details of the surface microscopic ordering.

Experimentally, the molecular orientation at the surface has been measured by optical second-harmonic-generation techniques [24]. Indeed, it has been found that it differs from the bulk orientation, determined by macroscopical measurements. The measured surface orientational distribution func-

tion on a rubbed polymer displays a rather large dispersion: this has been considered the source of the subsurface distortion and has been analyzed in terms of a Landau–de Gennes theory [24]. Our results cannot be directly compared to these data, as our orientational distribution function at the surface is different, being much more peaked around the easy axis. However, we have shown that various effects that cannot be accounted for in a standard Landau–de Gennes framework, play an important role. A competition between these effects yields strong subsurface distortions.

We thank H.-R. Trebin and M. Rasetti for the computing facilities. We are indebted also to C. Oldano, H.-R. Trebin, S. Faetti, and C. Zannoni for useful discussions. J.S. and L.L. gratefully acknowledge the EEC for financial support (Contracts No. ERBCHRXCT93019 and No. ERBCIPDCT940607, respectively).

-
- [1] J. Prost and P. G. de Gennes, *The Physics of Liquid Crystals* (Clarendon Press, Oxford, 1993).
- [2] C. W. Oseen, *Trans. Faraday Soc.* **29**, 883 (1933).
- [3] H. Zöcher, *Trans. Faraday Soc.* **29**, 945 (1933).
- [4] F. C. Frank, *Disc. Faraday Soc.* **25**, 19 (1958).
- [5] J. Nehring and A. Saupe, *J. Chem. Phys.* **54**, 337 (1971).
- [6] J. Nehring and A. Saupe, *J. Chem. Phys.* **56**, 5527 (1972).
- [7] C. Oldano and G. Barbero, *J. Phys. Lett. (Paris)* **46**, 451 (1985).
- [8] G. Barbero, N. V. Madhusudana, and C. Oldano, *J. Phys. (Paris)* **50**, 226 (1989).
- [9] H. P. Hinov, *Mol. Cryst. Liq. Cryst.* **148**, 197 (1987).
- [10] V. M. Pergamenschik, *Phys. Rev. E* **48**, 1254 (1993); **49**, 934 (1994).
- [11] J. G. Gay and B. J. Berne, *J. Chem. Phys.* **74**, 3316 (1981).
- [12] G. Barbero and C. Oldano, *Mol. Cryst. Liq. Cryst.* **170**, 99 (1989).
- [13] E. de Miguel and L. F. Rull, *Mol. Phys.* **74**, 405 (1991).
- [14] J. Stelzer, L. Longa, and H.-R. Trebin, *J. Chem. Phys.* **103**, 3098 (1995).
- [15] A. Rapini and M. Papoular, *J. Phys. Colloq. (Paris)* **30**, C4-54 (1969).
- [16] S. Toxvaerd, *Phys. Rev. E* **47**, 343 (1993).
- [17] T. J. Sluckin and A. Poniewierski, in *Fluid Interfacial Phenomena*, edited by C. A. Croxton (Wiley, New York, 1985).
- [18] G. Barbero and G. Durand, *J. Phys. II (France)* **1**, 651 (1991).
- [19] M. Nobili and G. Durand, *Phys. Rev. A* **46**, R6174 (1992).
- [20] A. Poniewierski and R. Holyst, *Phys. Rev. A* **38**, 3721 (1988).
- [21] J. Als-Nielsen, F. Christensen, and P. S. Pershan, *Phys. Rev. Lett.* **48**, 1107 (1982).
- [22] E. F. Gramsbergen and W. H. de Jeu, *J. Phys. (Paris)* **49**, 363 (1988).
- [23] M. Rajteri, G. Barbero, P. Galatola, C. Oldano, and S. Faetti, *Phys. Rev. E* **53**, 6093 (1996).
- [24] Xiaowei Zhuang, L. Marrucci, and Y. R. Shen, *Phys. Rev. Lett.* **73**, 1513 (1994).